3′-Phosphoadenosine 5′-Phosphate Accumulation Delays the Circadian System[1][OPEN]

Suzanne Litthauer,[a] Kai Xun Chan,[b] and Matthew Alan Jones[a,2]

[a]School of Biological Sciences, University of Essex, Colchester, Essex CO4 3SQ, United Kingdom
[b]Center for Plant Systems Biology, VIB, 9052 Ghent, Belgium

ORCID IDs: 0000-0003-0265-3315 (S.L.); 0000-0003-3554-7228 (K.X.C.); 0000-0002-3943-3968 (M.A.J.).

The circadian system optimizes cellular responses to stress, but the signaling pathways that convey the metabolic consequences of stress into this molecular timekeeping mechanism remain unclear. Redox regulation of the SAL1 phosphatase during abiotic stress initiates a signaling pathway from chloroplast to nucleus by regulating the accumulation of a metabolite, 3′-phosphoadenosine 5′-phosphate (PAP). Consequently, PAP accumulates in response to redox stress and inhibits the activity of exoribonucleases (XRNs) in the nucleus and cytosol. We demonstrated that osmotic stress induces a lengthening of circadian period and that genetically inducing the SAL1-PAP-XRN pathway in plants lacking either SAL1 or XRNs similarly delays the circadian system. Exogenous application of PAP was also sufficient to extend circadian period. Thus, SAL1-PAP-XRN signaling likely regulates circadian rhythms in response to redox stress. Our findings exemplify how two central processes in plants, molecular timekeeping and responses to abiotic stress, can be interlinked to regulate gene expression.

The rotation of the Earth confers overt environmental rhythms upon species living on its surface. Both temperature and incident light change dramatically (yet predictably) over any given 24-h cycle, and as a consequence there is a selective pressure for species to anticipate changes in environmental conditions (Hut and Beersma, 2011). This selective pressure has led to the evolution of the circadian clock, an endogenous biological oscillator that modulates biochemical and physiological activity to optimize behavior within the prevailing environmental context (Millar, 2016).

The pervasive nature of the circadian system has encouraged the detailed description of the network underpinning these biological rhythms. Circadian rhythms are entrained to the local day/night cycle by regular changes in temperature and light (Jones, 2009; Hsu and Harmer, 2014). Phytochromes act to input red light-derived signals, while cryptochromes and the ZEITLUPE (ZTL) family are the predominant blue photoreceptors that influence circadian rhythms (Fankhauser and Staiger, 2002; Hsu and Harmer, 2014). Nuclear circadian rhythms within Arabidopsis (*Arabidopsis thaliana*) consist of multiple, interconnected transcriptional feedback loops (Hsu and Harmer, 2014). PSEUDORESPONSE REGULATOR9 (PRR9) acts sequentially with PRR7, PRR5, and PRR1/TIMING OF CAB EXPRESSION1 (TOC1) to repress expression of *CIRCADIAN CLOCK ASSOCIATED1* (*CCA1*) and *LATE ELONGATED HYPOCOTYL* (*LHY*) throughout the day (Farré and Kay, 2007; Nakamichi et al., 2010; Gendron et al., 2012; Huang et al., 2012). In turn, CCA1 and LHY (whose expression is induced by light at dawn) repress expression of *PRR9/7/5/TOC1* (Alabadí et al., 2001; Adams et al., 2015) and additional circadian genes such as *GIGANTEA* (Lu et al., 2012). Subsequently, a complex of proteins, including EARLY FLOWERING4 (ELF4), act to repress circadian gene expression during the early night (McWatters et al., 2007; Nusinow et al., 2011; Chow et al., 2012; Herrero et al., 2012). The oscillations generated by these feedback loops modulate many physiological processes including growth, photosynthesis, flowering time, and responses to biotic and abiotic stresses (Dong et al., 2011; Eriksson and Webb, 2011; Hsu and Harmer, 2014; Song et al., 2015; Jones, 2017).

We have been interested in the molecular interactions between plants' response to stress and the circadian system so as to improve survival. Damage induced by abiotic factors is typically first observed within the chloroplast and mitochondria, where perturbations in metabolism rapidly induce oxidative damage (Mittler et al., 2011). These perturbations are communicated from organelles to the nucleus via multiple retrograde signaling pathways that adjust nuclear gene expression. However, the extent to which retrograde

[1] This work was supported by the Leverhulme Trust (ECF-2012-358), The Royal Society (grant no. RG130746), The Oppenheimer Memorial Trust (PhD studentship to S.L.), The Gen Foundation (to S.L.), the University of Essex, and the Australian Research Council Centre of Excellence in Plant Energy Biology (CE140100008).

[2] Address correspondence to matthew.jones@essex.ac.uk.

The author responsible for distribution of materials integral to the findings presented in this article in accordance with the policy described in the Instructions for Authors (www.plantphysiol.org) is: Matthew Alan Jones (matthew.jones@essex.ac.uk).

S.L. and M.A.J. performed the research and analyzed data; S.L., K.X.C., and M.A.J. designed the research and wrote the article.

[OPEN] Articles can be viewed without a subscription.

www.plantphysiol.org/cgi/doi/10.1104/pp.17.01611

signals can regulate plant homeostasis, and by what mechanism(s), remain enigmatic (Chan et al., 2016b). We therefore examined a candidate signaling pathway that could be responsible for coordinating nuclear circadian rhythms in response to metabolic stress in the chloroplast. SAL1 is a redox-sensitive phosphatase localized to the chloroplast and mitochondria (Chen et al., 2011; Estavillo et al., 2011; Chan et al., 2016a). A recent model of SAL1-initated signaling from chloroplast to nucleus has proposed that upon oxidative stress, redox-induced impairment of SAL1 activity leads to accumulation of its substrate 3′-phosphoadenosine 5′-phosphate (PAP), resulting in inhibition of 5′→3′ exoribonuclease (XRN) activity and subsequent changes in expression of plastid redox-associated nuclear genes and abscisic acid (ABA) signaling (Dichtl et al., 1997; Mechold et al., 2006; Estavillo et al., 2011; Chan et al., 2016a; Pornsiriwong et al., 2017). This model is supported by analysis of the transcriptomes of *xrn* and *sal1* mutants, with considerable overlap between the misregulated transcripts in each of these genotypes (Gy et al., 2007; Estavillo et al., 2011; Kurihara et al., 2012). In this study, we demonstrated that osmotic stress delays the circadian system and that constitutive activation of PAP signaling in *sal1* and *xrn* plants results in an extended circadian period. These data provide an additional mechanism through which the molecular clock, a cornerstone of plant function, can be coordinated with the metabolic status of a plant cell to guide molecular responses to environmental fluctuations.

RESULTS

Whole-Plant Osmotic Stress Treatments Lengthen Circadian Period and Induce Accumulation of PAP

Drought is a multifaceted stress that arises from limited water availability and is one of the primary abiotic stresses that limits crop yield (Verslues et al., 2006; Steduto et al., 2012). We therefore sought to understand how this stress affects the circadian system using the model plant Arabidopsis. As consistent maintenance of soil water potential during circadian imaging presented technical issues, we instead approximated the physiological consequences of water deficit stress through the addition of 200 mM mannitol to lower the water potential of the agar substrate (Fig. 1; Verslues et al., 2006). One of the initial metabolic consequences of water-deficit stress is the accumulation of PAP due to the redox-induced inactivation of SAL1 (Estavillo et al., 2011; Chan et al., 2016b), so we measured PAP levels under our experimental conditions. As previously reported for soil-grown plants, the application of osmotic stress was sufficient to induce accumulation of PAP, with comparable increases in PAP observed in plants transferred to mannitol and grown under either constant white (cW) light or constant red +blue light provided by LEDs (cR+B; Fig. 1A; Estavillo et al., 2011). Interestingly, we observed a 1-h increase in the circadian free running period (FRP) in wild-type plants subjected to osmotic stress under cR+B light (Fig. 1, B and C; $P < 0.01$, Dunnett's test). A comparable FRP extension of approximately 1 h was observed in plants transferred to Murashige and Skoog (MS) plates infused with an alternate osmoticum (PEG 8000; Fig. 1, B and C).

Loss of SAL1 Activity Results in Lengthening of Circadian Period in *sal1* Mutants

We hypothesized that the accumulation of PAP during osmotic stress contributed to the observed extension of the circadian period. Intracellular PAP accumulation can be increased through disruption of *SAL1*, a gene that encodes a redox-sensitive phosphatase, so we examined the FRP of *sal1* mutant alleles to test our hypothesis (Fig. 2; Kim and von Arnim, 2009; Wilson et al., 2009; Rodríguez et al., 2010). Circadian rhythms can be routinely monitored by measuring changes in photosystem II (PSII) operating efficiency (F_q'/F_m'; Litthauer et al., 2015). Using this technique, we observed a significant increase in FRP under constant blue (cB) light in *alx8-1*, *fry1-6*, and *fou8* alleles of *SAL1* compared to the wild type (Fig. 2, A–D; Supplemental Fig. S1). This long-period phenotype was rescued by introducing a wild-type copy of the *SAL1* coding region along with a 1-kb region of upstream genomic sequence into the *alx8-1* background (Fig. 2E), suggesting that a mutation in *SAL1* underlies the phenotype observed in the mutant lines.

To better document the *sal1* mutant circadian phenotype, we introduced a *CCA1::LUC2* luciferase reporter into the *fry1-6* background (Fig. 2F). When measuring luciferase bioluminescence, we observed a 1-h extension of FRP under cB light (23.80 ± 0.17 h in the wild type compared to 25.23 ± 0.14 h in *fry1-6*; $P < 0.025$, Student's *t* test). We also observed a modest yet significant increase in FRP under cR+B light (22.90 ± 0.05 h in the wild type compared to 23.52 ± 0.07 h in *fry1-6*, $P < 0.05$, Student's *t* test; Fig. 2F). Interestingly, we did not observe a difference in FRP between wild-type and *sal1* plants under constant red (cR) light or constant darkness (Fig. 2F). Such data suggest that FRP is delayed in a blue light-dependent manner in *sal1* mutants.

PAP accumulates in vivo in response to osmotic stress due to a change in the redox state within the chloroplast that inhibits the enzymatic activity of SAL1 (Chan et al., 2016a). We therefore sought to assess the consequences of these oxidative stresses upon the nuclear circadian system (Fig. 2G). We first used 50 μM methyl viologen (MV; which induces reactive oxygen species production at PSII) to induce oxidative stress within the chloroplast (Fig. 2G; Lai et al., 2012; Chan et al., 2016a). Application of MV induced a 1.5-h lengthening of circadian period in wild-type seedlings (τ = 22.66 ± 0.08 and 24.25 ± 0.15 h on mock- and

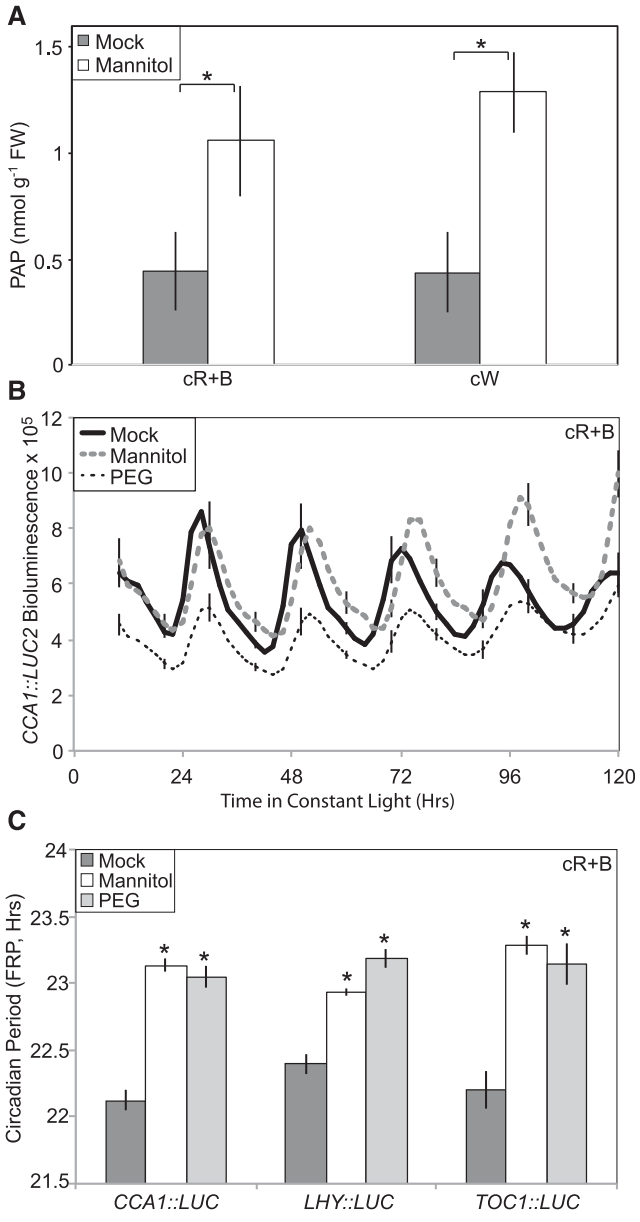

Figure 1. Osmotic stress induces the accumulation of PAP and extends the circadian period. A, Accumulation of PAP in Columbia (Col-0) seedlings in the presence of 200 mM mannitol under constant light conditions. Plants were grown for 11 d under 12/12-h light/dark (L/D) cycles before being transferred to plates containing 200 mM mannitol 24 h before transfer to constant light. Plates were transferred to either 24 μmol m^{-2} s^{-1} constant blue light supplemented with 36 μmol m^{-2} s^{-1} red light (cR+B) or to 60 μmol m^{-2} s^{-1} constant white light (cW) at dawn of day 12. Seedlings were harvested at ZT96. Data are the mean of three biological replicates and are representative of two independent experiments. Error bars indicate SD. Asterisks indicate a significant difference compared with the respective mock control ($P < 0.025$, Bonferroni adjusted Student's t test). B, Representative bioluminescence data of luciferase activity in Col-0 plants carrying a *CCA1::LUC2* reporter construct in the presence of 200 mM mannitol or PEG 8000. Plants were grown on half-strength MS medium for 5 d under 12/12-h L/D cycles before being transferred to either a mock-treated control, 200 mM mannitol, or plates infused with PEG 8000 24 h before imaging under cR+B light (30 μmol m^{-2} s^{-1} red and 20 μmol m^{-2} s^{-1} blue light). Data are representative of three independent experiments. Error bars represent SE and are presented every 10 h for clarity. $n = 10$. C, Circadian period estimates of luciferase activity in the presence of 200 mM mannitol or PEG 8000. Col-0 seedlings carrying either the *CCA1*, *LHY*, or *TOC1* promoters fused to a *LUCIFERASE* reporter were assessed. Data are representative of three independent experiments. Error bars express SE, $n = 10$. Asterisks indicate $P < 0.01$ compared with mock controls (Dunnett's test).

MV-treated plates, respectively), with a more modest lengthening observed in *fry1-6* seedlings (τ = 23.23 ± 0.21 and 24.57 ± 0.16 h in the absence or presence of MV, respectively). Intriguingly, FRP in wild-type and *sal1* seedlings was indistinguishable after MV treatment. Therefore, the application of oxidative stress using MV lengthens circadian period.

Recent work has suggested that PAP acts as a secondary messenger during ABA signaling to promote stomatal closure (Pornsiriwong et al., 2017), and so we next examined whether exogenous ABA was able to reconstitute the long-period phenotype of *sal1* plants (Fig. 2H). In contrast to our hypothesis, the circadian FRP was reduced in both wild-type and *sal1* plants in the presence of exogenous ABA when compared to mock-treated controls (Fig. 2H). In the presence of ABA, *sal1* lines retained their extended FRP phenotype (posthoc Bonferroni adjusted t test), although the magnitude of the phenotype was less than in mock-treated plants (Fig. 2H). Our data suggest that enhanced ABA signaling does not contribute to the delayed FRP of *sal1* plants, although additional work will be required to fully understand the interaction between SAL1 and ABA signaling in a circadian context.

It has been proposed that increased fluence rates enhance the accumulation of PAP in vivo (Estavillo et al., 2011); therefore, we completed fluence rate response curves under either cB or cR light to determine whether increased fluence rates would exacerbate the *sal1* circadian phenotype (Fig. 3). Under dim blue light (5 μmol m^{-2} s^{-1}), we did not observe a difference in FRP between wild-type and *fry1-6* plants (Fig. 3A). However, we did observe a significant difference in *sal1* plants' response to increasing blue light compared to the wild type ($P < 0.001$), which resulted in a lengthening of FRP in *sal1* plants transferred to ≥20 μmol m^{-2} s^{-1} cB light (Fig. 3A). By contrast, we did not observe a significant lengthening of FRP in *fry1-6* plants transferred to any tested fluence rate of cR light, as was suggested by our initial studies under cR light (Figs. 2F and 3B).

In order to better understand the extended circadian FRP phenotype, we examined the accumulation of clock-regulated transcripts under either 20 μmol m^{-2} s^{-1} blue light or 30 μmol m^{-2} s^{-1} red light (Fig. 3, C–F; Supplemental Fig. S2). In agreement with our luciferase data (Figs. 2F and 3, A and B), we observed that *CCA1* and *TOC1* transcript accumulation was delayed by ~6 to 9 h under cB light (Fig. 3, C and E). This phase shift

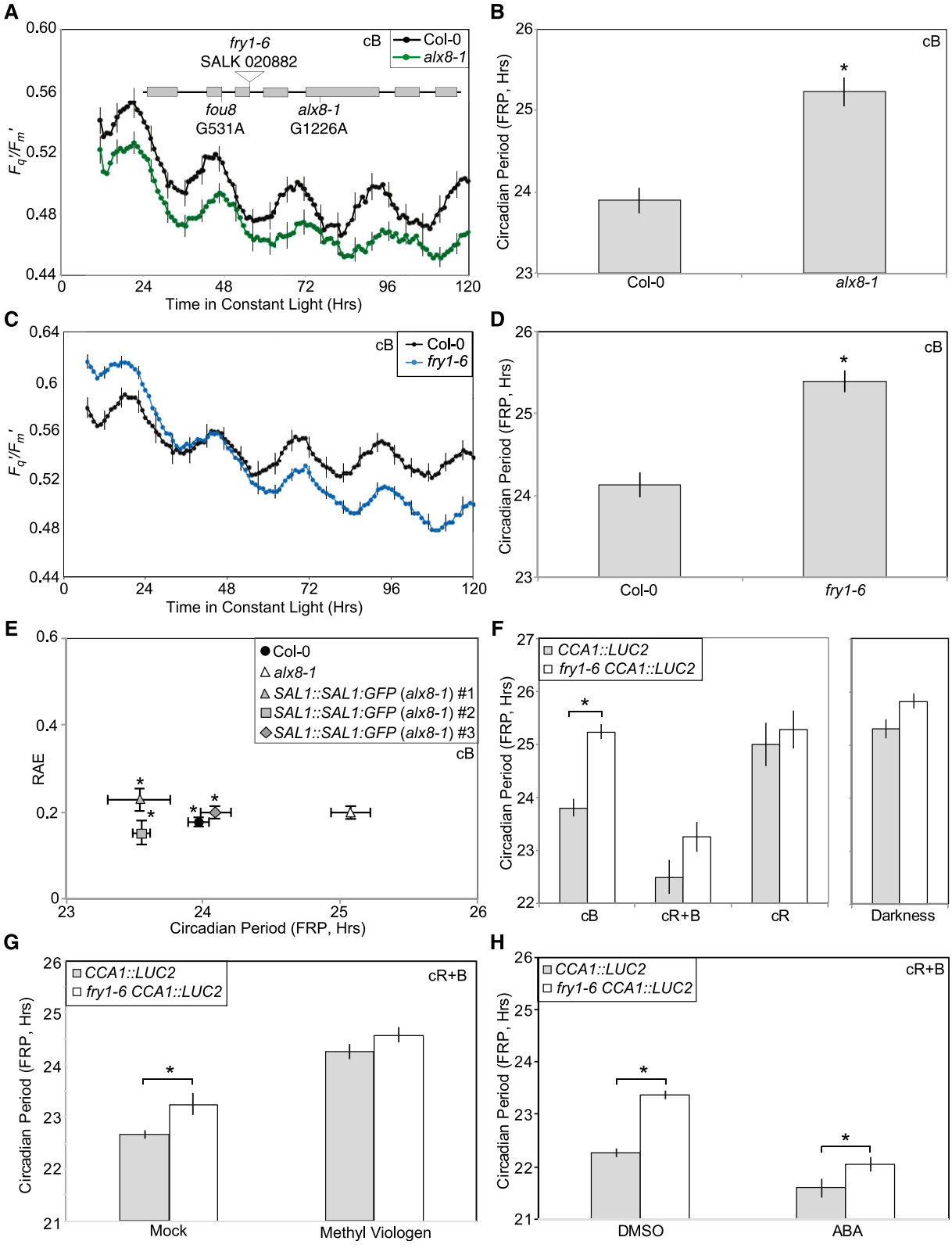

Figure 2. *sal1* alleles have an extended circadian period. A and C, Rhythms of PSII operating efficiency (F_q'/F_m') measured over circadian time in *alx8-1* (A) and *fry1-6* (C) mutant alleles of *SAL1*. Plants were grown for 12 d under 12/12-h L/D cycles before being transferred to constant blue light (20 μmol m^{-2} s^{-1}). Data represent mean values of multiple seedlings (n = 8) and are representative of at least three independent experiments. SE is presented every 5 h for clarity. B and D, Circadian period estimates

was less apparent in plants transferred to cR light (Fig. 3, D and F). Since *sal1* plants present a blue light-dependent phenotype, we monitored the accumulation of *CRYPTOCHROME1* (*CRY1*), *CRY2*, and *ZEITLUPE* transcripts to confirm that accumulation of these blue photoreceptors was not repressed by the loss of *SAL1*. However, we found that neither *CRY1*, *CRY2*, nor *ZEITLUPE* transcript accumulation was significantly repressed in *sal1* plants (Supplemental Fig. S3).

We next examined PAP accumulation in plants grown under our experimental light conditions. As previously reported, we were unable to detect PAP in any of our wild-type samples (Fig. 3, G and H; Chen et al., 2011; Estavillo et al., 2011; Lee et al., 2012). In *fry1-6* plants, the absence of a circadian phenotype under lower cB light intensities was correlated with a significant reduction in PAP accumulation (Fig. 3G), with <2 nmol g^{-1} PAP accumulating in *fry1-6* plants under dim blue light compared to in excess of 5 nmol g^{-1} above 20 μmol m^{-2} s^{-1} blue light (Fig. 3G). Interestingly, PAP accumulation remained greater in *fry1-6* plants transferred to different intensities of cR or cR+B despite the circadian phenotype being less pronounced under these conditions (Fig. 3, H and I; Supplemental Fig. S4). Such data suggest that PAP acts to delay the circadian system via a blue light-induced pathway or that cR light stimulates an opposing or compensatory signaling cascade.

Reduced PAP Accumulation Rescues the Circadian Phenotype of *sal1* Mutants

Loss of SAL1 activity results in a lengthened circadian phenotype (Fig. 2), so we examined whether PAP levels correlated with FRP in *sal1* mutants (Fig. 4). Given the correlation between PAP accumulation and the *sal1* circadian phenotype under cB light, we hypothesized that exogenous application of PAP would be sufficient to extend FRP. Application of PAP to intact wild-type seedlings did not induce gene expression, presumably because of the enzymatic activity of the endogenous SAL1 protein (Estavillo et al., 2011; Pornsiriwong et al., 2017). Therefore, we examined whether the application of additional PAP was sufficient to extend FRP in *sal1* plants that have a compromised ability to degrade exogenous PAP (Fig. 4A). Following entrainment, plants were transferred to cB light for imaging before PAP was applied. As expected, there was no significant difference in FRP in wild-type plants following PAP application ($P = 0.953$; Fig. 4A). However, we did observe a lengthening of circadian periodicity from 24.52 ± 0.14 h to 25.25 ± 0.12 h in *sal1* plants following treatment with PAP (Fig. 4A; $P < 0.025$).

We next tested whether reduced PAP accumulation in the *sal1* background was sufficient to rescue the circadian phenotype (Fig. 4, B–D). SAL1 is a bifunctional enzyme with PAP phosphatase and inositol polyphosphate 1-phosphatase activities in vitro (Quintero et al., 1996; Xiong et al., 2001). In order to specifically reduce PAP levels in vivo, we overexpressed *ARABIDOPSIS HAL2-LIKE* (*AHL*), a paralog of *SAL1* with only PAP phosphatase activity (Kim and von Arnim, 2009; Chen and Xiong, 2010; Hirsch et al., 2011). Transgenic lines overexpressing *AHL* in an *alx8-1* background had wild-type levels of PAP under cB light (Fig. 4B). We also found that overexpression of the *AHL* paralog was able to rescue the mutant circadian phenotype of *alx8-1* seedlings (Fig. 4, C and D). Such data demonstrate that PAP phosphatase activity is sufficient to reduce PAP accumulation and complement the *sal1* circadian phenotype.

SAL1 Is a Constitutively Expressed Protein

As *sal1* mutants have not previously been characterized as having a circadian phenotype, we explored the regulation of *SAL1* transcripts and protein over diel

Figure 2. (*Continued.*)
of F_q'/F_m' circadian rhythms presented in A and C using FFT-NLLS with baseline detrending (Plautz et al., 1997). Asterisks indicate a significant difference compared with the Col-0 control ($P < 0.05$, Student's *t* test). E, Circadian period estimates of F_q'/F_m' circadian rhythms in Columbia (Col-0), *alx8-1*, and *alx8-1* seedlings transformed with a *SAL1::SAL1-GFP* construct. Period estimates are plotted against RAE, which is a measure of rhythmic robustness (a value of 0 indicates an exact fit to a cosine wave; Plautz et al., 1997); $n = 8$. Data from one of three independent experiments are shown. Asterisks indicate a significant difference compared with the *alx8-1* mutant ($P < 0.05$, Dunnett's test). F, Circadian period estimates of luciferase activity in Columbia (Col-0) and *fry1-6* plants carrying a *CCA1::LUC2* reporter construct. Plants were grown on half-strength MS medium for 6 d before transfer to either 20 μmol m^{-2} s^{-1} blue light (cB), a combination of 30 μmol m^{-2} s^{-1} red light and 20 μmol m^{-2} s^{-1} blue light (cR+B), or 30 μmol m^{-2} s^{-1} red light (cR). Plants transferred to constant darkness (Darkness) were grown on half-strength MS medium supplemented with 3% (w/v) Suc. Data are representative of at least three independent experiments. Error bars express SE, $n = 10$. Asterisks indicate a significant difference compared with the Columbia control ($P < 0.025$, Bonferroni adjusted Student's *t* test). G, Circadian period estimates of luciferase activity in Columbia (Col-0) and *fry1-6* plants carrying a *CCA1::LUC2* reporter construct in the presence of methyl viologen. Plants were grown on half-strength MS medium for 6 d before application of 50 μM methyl viologen and transfer to 20 μmol m^{-2} s^{-1} blue light and 30 μmol m^{-2} s^{-1} red light for imaging. Data are representative of three independent experiments. Error bars express SE, $n = 10$. Asterisks indicate $P < 0.025$ compared with the respective Columbia control (posthoc Bonferroni adjusted Student's *t* test). H, Circadian period estimates of luciferase activity in the presence of 10 μM ABA. Data are representative of three independent experiments. Error bars express SE, $n = 10$. Asterisks indicate a significant difference compared with indicated controls ($P < 0.025$, posthoc Bonferroni adjusted Student's *t* test).

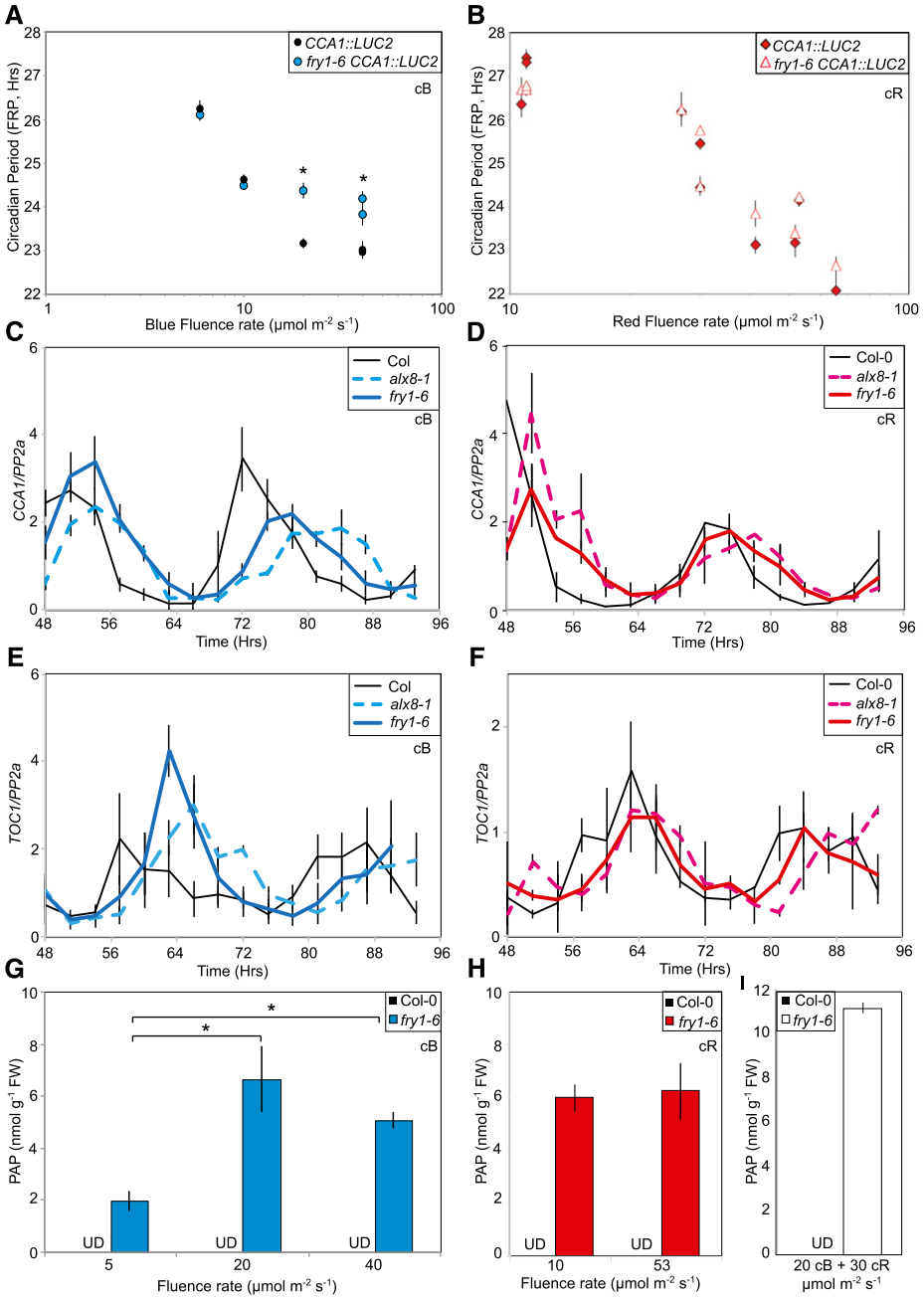

Figure 3. The *sal1* circadian phenotype is exacerbated under blue light. A, Fluence rate response curves to measure the free-running circadian period under cB light in Col-0 and *fry1-6* seedlings carrying a *CCA1::LUC2* reporter. Seedlings were entrained in 12/12-h L/D cycles for 6 d before being transferred to the indicated fluence rate of cB light. Data are representative of three independent experiments; SE is shown, $n = 10$. Asterisks highlight a significant difference between Col-0 and *fry1-6* at the indicated fluence rate (posthoc Student's *t* test, $P < 0.05$). B, Fluence rate response curves to measure the free-running circadian period under cR light. Seedlings were entrained as described in A before being transferred to the indicated fluence rate of constant red light. Data are representative of three independent experiments; SE is shown, $n = 10$. C to F, Accumulation of circadian clock-regulated transcripts under cB (C and E) or cR (D and F) light in *sal1* seedlings using RT-qPCR. Levels of *CCA1* (C and D) and *TOC1* (E and F) mRNA were assessed. Plants were entrained to 12/12-h L/D cycles for 12 d on MS medium before being moved to constant conditions with either 20 μmol m^{-2} s^{-1} blue (cB) or 30 μmol m^{-2} s^{-1} red (cR) light. Data for each gene were normalized with an internal control (*PP2a*) and are the mean of at least two biological replicates. Error bars indicate SE. G to I, Accumulation of PAP in *fry1-6* seedlings under different fluence rates of blue (G), red (H), or red+blue (I) light. Seedlings were entrained in 12/12-h L/D cycles for 12 d before being transferred to the indicated fluence rate and quality of light for 4 d. Seedlings were harvested at ZT96. UD, PAP levels were below the detection threshold in Col-0 in each measurement. Asterisks highlight a significant difference for the selected comparison ($P < 0.025$, Bonferroni adjusted Student's *t* test).

and circadian timescales (Fig. 5). Consistent with previous microarray studies (Supplemental Fig. S5; Mockler et al., 2007), we found that *SAL1* transcripts accumulate gradually over the course of the day under entraining conditions (Fig. 5A), whereas under cW light, we did not observe a discernible rhythm in *SAL1* transcript (Fig. 5C; Mockler et al., 2007). Interestingly, no changes in protein accumulation were apparent in our transgenic lines expressing *SAL1-GFP* under the control of its native promoter (Fig. 5B). *SAL1* oscillations consequently appear to be primarily driven by the diel cycle rather than *SAL1* being a classical output of the core nuclear circadian system.

Lengthening of Circadian Period in *sal1* Mutants Is Not Induced by Sulfur Deprivation

The *sal1* mutation induces accumulation of its substrate, PAP, and to a lesser extent the PAP precursor, 3′-phosphoadenosine 5′-phosphosulfate (PAPS; Fig. 6; Chen et al., 2011; Estavillo et al., 2011; Lee et al., 2012). As a consequence, *sal1* seedlings present a sulfur-deprived phenotype, presumably derived from disruption of sulfate assimilation pathways (Fig. 6A; Mugford et al., 2009; Lee et al., 2012). Sulfate assimilation is vital for plant metabolism (Takahashi et al., 2011), so we investigated whether the long-period circadian phenotype of the *sal1* mutant is induced via the reduced accumulation of sulfate. We first evaluated the consequences of gross sulfate starvation on nuclear rhythms using a collection of luciferase reporter lines in a wild-type background (Fig. 6B; Supplemental Fig. S6). Our sulfate-deprived growth conditions were sufficient to induce accumulation of the sulfate starvation marker *APS REDUCTASE1* and *SULTR4;2* (Supplemental Fig. S6). However, despite the induction of a sulfate starvation response, there was no difference in the period of bioluminescence rhythms driven by the *CCA1*, *LHY*, or *TOC1* promoters (Fig. 6B; Supplemental Fig. S6, B–D). As sulfates are necessary for the maintenance of photosynthesis (Terry, 1976), we next examined rhythms of PSII operating efficiency in wild-type and *fry1-6* plants under sulfate-deprived conditions (Fig. 6C; Supplemental Fig. S6E). As with our studies using luciferase reporters (Fig. 6B), we did not observe any significant difference in FRP in wild-type plants in the presence or absence of sulfates (τ = 23.96 ± 0.32 and 23.74 ± 0.30 h on MS media and MS media lacking sulfates, respectively). Sulfate deprivation is therefore insufficient to extend the period of the circadian system.

In order to further evaluate the contribution of sulfur limitation to the *sal1* circadian phenotype, we examined additional mutant lines deficient in sulfate metabolism (Fig. 6, A, D, and E). Plants lacking *ARABIDOPSIS 5-PHOSPHOSULFATE KINASE1* (*APK1*) and *APK2* are less able to phosphorylate adenosine 5′-phosphosulfate and so accumulate fewer glucosinolates, with a commensurate increase in desulfo-glucosinolates, a phenotype that is also observed in *sal1* alleles (Mugford et al., 2009; Lee et al., 2012). When we examined plants grown on sulfate-deficient media, we observed no difference in FRP in *apk1 apk2* mutants compared to the wild type (Fig. 6D; τ= 23.87 ± 0.11 h in *apk1 apk2* compared to 23.70 ± 0.09 h in the wild type). Similarly, *cad2-1* plants, which accumulate less glutathione than wild-type plants (Cobbett et al., 1998), had a comparable phenotype to wild-type plants (Fig. 6E). These data demonstrate that gross deficiencies in sulfate metabolism do not extend FRP and thus are unlikely to account for the mechanism by which SAL1/PAP signaling regulates the circadian rhythm.

Plants Lacking Exoribonucleases Have a Comparable Long-Period Phenotype to the *sal1* Mutant

The accumulation of PAP as a consequence of *SAL1* inactivation leads to the inhibition of XRN exoribonuclease activity (Chan et al., 2016b). As misregulation of RNA processing frequently leads to an altered circadian free-running period (Jones et al., 2012; Wang et al., 2012; MacGregor et al., 2013; Perez-Santángelo et al., 2014), we examined whether a mutation of XRN exoribonucleases to genetically simulate SAL1-mediated XRN inhibition was sufficient to alter nuclear circadian rhythms (Fig. 7).

The Arabidopsis genome expresses three *XRN* genes, with XRN2 and XRN3 acting within the nucleus whereas XRN4 accumulates in the cytosol (Kastenmayer and Green, 2000). Transcripts from these genes did not accumulate with a daily rhythm (Supplemental Fig. S5). As XRNs display a degree of functional redundancy and are likely all inhibited by PAP accumulation (Gy et al., 2007; Nagarajan et al., 2013), we examined circadian rhythms in the *xrn2 xrn3 xrn4* (*xrn234*) triple mutant (Fig. 7). As observed in *sal1* plants, these *xrn234* seedlings have a long FRP compared to the wild type (Fig. 7A; τ = 24.71 ± 0.20 h in *xrn234* compared to 23.88 ± 0.19 h in the wild type). This long-period phenotype corresponded to a delayed phase of *CCA1* transcript accumulation under cB light in both *fry1-6* and *xrn234* seedlings (Fig. 7B). Interestingly, this phase delay in transcript accumulation in *xrn234* seedlings was less apparent in cW light, similar to the more subtle phenotype observed in *sal1* alleles under cW light or cR+B light (Figs. 2F and 7C). These data support the current model for PAP signaling that suggests that PAP accumulation in *sal1* lines represses XRN activity, rather than direct targeting of individual transcripts (Wilson et al., 2009; Rodríguez et al., 2010; Lee et al., 2012).

Loss of SAL1 Mimics the Clock's Response to Osmotic Stress via a Blue Light-Induced Pathway

In order to assess the contribution of SAL1 and PAP to circadian timekeeping during osmotic stress, we revisited our experimental design outlined in Figure 1. The transfer to media containing mannitol did not induce the accumulation of additional PAP in *sal1* plants under either cR+B or cB light, although PAP accumulation increased in the wild type as previously observed (Figs. 1A and 8, A and B). Under cR+B light, *sal1* seedlings had a

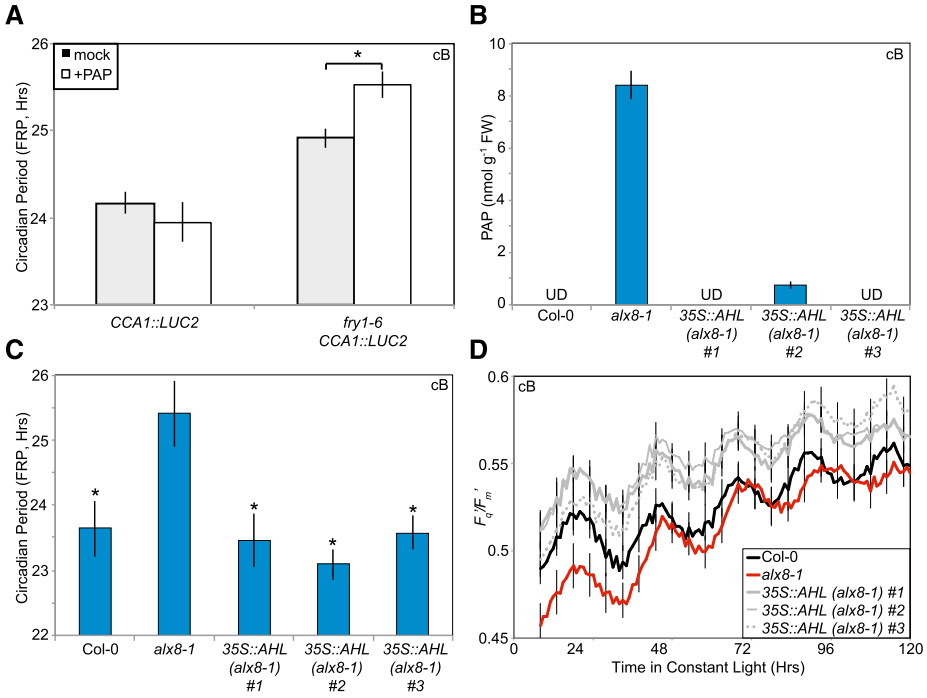

Figure 4. PAP accumulation is correlated with circadian defects in *sal1* mutants. A, Circadian period of *fry1-6* seedlings following application of PAP. Seedlings were entrained in 12/12-h L/D cycles for 6 d before being transferred to 20 μmol m^{-2} s^{-1} cB light. PAP was applied at ZT29. Asterisks indicate a significant difference compared with the mock-treated control ($P < 0.025$, Bonferroni adjusted Student's *t* test). SE is shown, $n > 19$. Data are representative of three independent experiments. B, Accumulation of PAP in Col-0, *alx8-1*, and *alx8-1* seedlings transformed with a *35S::AHL* construct. Plants were grown for 12 d under 12/12-h L/D cycles before being transferred to constant 20 μmol m^{-2} s^{-1} blue (cB) light. Seedlings were harvested at ZT96. Data are the mean of three biological replicates and are representative of two independent experiments. UD, PAP levels were below the detection threshold. C and D, F_q'/F_m' rhythms and circadian period estimates in *alx8-1* seedlings transformed with a *35S::AHL* construct. Plants were grown for 12 d under 12/12-h L/D cycles before being transferred to cB light (20 μmol m^{-2} s^{-1}). Data are representative of three independent experiments; SE is shown, $n = 8$. Asterisks indicate a significant difference compared with *alx8-1* plants ($P < 0.0125$, Bonferroni adjusted Student's *t* test).

longer FRP than wild-type controls in the presence or absence of mannitol, which correlated with the increased accumulation of PAP in these lines (Fig. 8C). Both wild-type and *sal1* plants retained a modest (yet significant) circadian response to osmotic stress under cR+B and cR light (Fig. 8C; Supplemental Fig. S7). Interestingly, *sal1* seedlings did not have an extended circadian FRP when transferred to mannitol under cB light, although wild-type plants retained this response (Fig. 8D). Comparable mannitol-induced shifts in circadian phase were observed when we examined the accumulation of *CCA1*, *PRR5*, and *GI* transcripts under cB light (Fig. 8E; Supplemental Fig. S8). Such data suggest that PAP accumulation is sufficient to extend circadian FRP under cB light but that additional red light-induced factors also coordinate the circadian system's response to mannitol.

DISCUSSION

PAP Accumulation Is Sufficient to Extend Circadian Period in the Presence of Blue Light

Inactivation of SAL1 through either mutation or application of oxidative stress within the chloroplast induces the accumulation of PAP (Estavillo et al., 2011; Chan et al., 2016). We were able to detect PAP in *sal1* seedlings under all conditions tested, but only observed an extension of circadian FRP under cB or cR+B light (Figs. 1, 3, 4, and 8). PAP accumulated to a greater extent in *sal1* seedlings transferred to 20 or 40 μmol m^{-2} s^{-1} cB light compared to those moved to 5 μmol m^{-2} s^{-1} cB light (Fig. 3G). This increase in PAP accumulation was correlated with the presentation of the mutant circadian phenotype, with *sal1* seedlings having an FRP indistinguishable from the wild type when transferred to very dim blue light (Fig. 3A). Despite this correlation, PAP levels remained higher in *sal1* mutants than in the wild type under these low light conditions (Fig. 3G). Such data suggest that either a threshold concentration of PAP is necessary in vivo to delay the molecular clock or that the blue light-dependent signal perturbed by PAP is only significant at higher fluence rates of blue light.

Intriguingly, we also noted that *sal1* and *xrn234* seedlings had a less pronounced circadian defect when transferred to constant conditions that included red wavelengths of light (Figs. 2F, 7, and 8), although elevated PAP levels were also observed in *sal1* plants transferred to cR light (Fig. 3H; Supplemental Fig. S4).

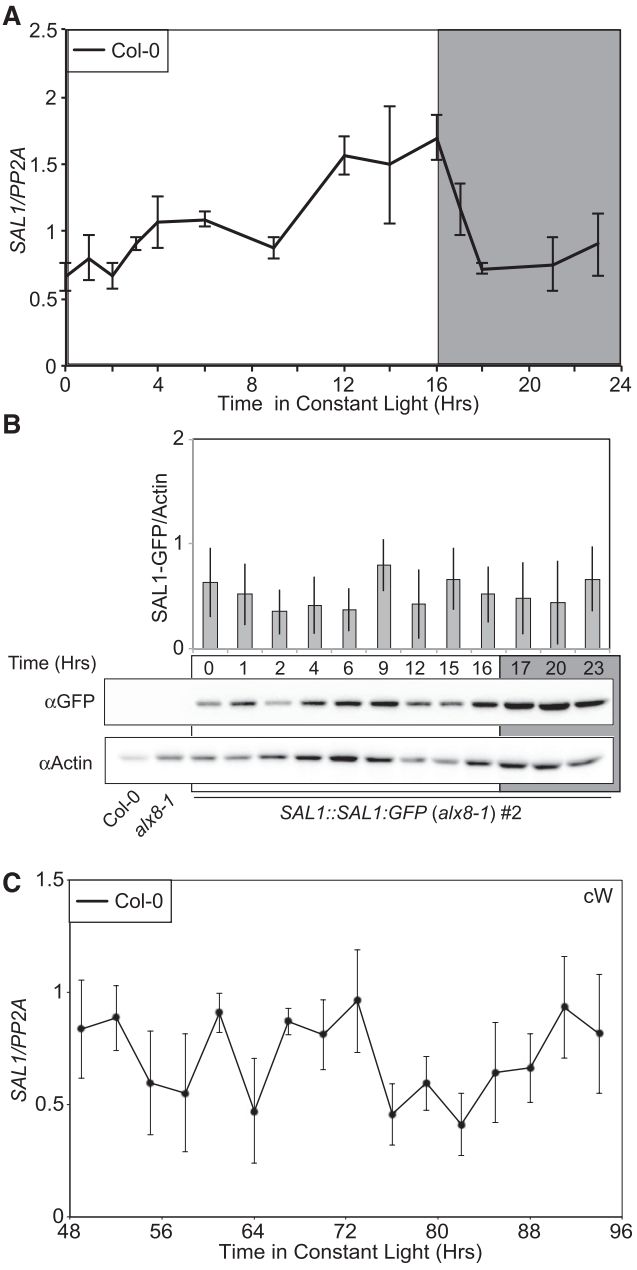

Figure 5. *SAL1* transcript and protein accumulation are not altered by the circadian system. A, *SAL1* transcript accumulation in Col-0 plants under 16/8-h L/D cycles. Data were normalized to an internal control (*PP2a*). Data are the average of three biological replicates; error bars show SE. B, Immunoblot analysis of SAL1 protein levels under 16/8-h LD cycles. Plants were grown as described in A. Data are the average of three biological replicates; error bars show SE. C, *SAL1* transcript accumulation over circadian time. Col-0 plants were entrained under 60 μmol m^{-2} s^{-1} white light in 12/12-h L/D cycles for 12 d before being transferred to cW light. Data are the mean of three biological replicates. Error bars express SE.

Such data suggest that either a red light-mediated signal supersedes or acts in parallel with the PAP-derived pathway or that the PAP-derived signal specifically affects a blue light-mediated response. The role of phytochrome-related factors in chloroplast retrograde signaling has previously been demonstrated (Salomé et al., 2013; Norén et al., 2016). Plants lacking iron have an extended FRP that is dependent upon phytochromes, suggesting an additional role for iron within the circadian system beyond the maintenance of photosynthesis (Chen et al., 2013; Hong et al., 2013; Salomé et al., 2013). As a consequence, it is likely that multiple signals relay information regarding the metabolic status of the chloroplast to the nucleus.

Exogenous applications of PAP alone to intact leaves of wild-type plants has previously been shown to be ineffective, presumably because endogenous SAL1 is sufficient to metabolize this exogenous PAP (Estavillo et al., 2011; Pornsiriwong et al., 2017). However, the exogenous application of PAP was sufficient to extend FRP in *fry1-6* seedlings (Fig. 4A). The exogenous application of PAP is therefore sufficient to extend the long-period circadian phenotype of *sal1* mutant plants that are unable to degrade this metabolite, suggesting that accumulation of PAP underlies the circadian phenotype of *sal1* plants.

Mutation of *SAL1* has a pleiotropic effect upon plant development, with auxin hyposensitivity and ABA hypersensitivity being reported in *sal1* alleles (Xiong et al., 2001; Chen and Xiong, 2010; Rodríguez et al., 2010). In particular, the accumulation of PAP in *sal1* plants up-regulates specific ABA signaling components to induce stomatal closure (Pornsiriwong et al., 2017). ABA induces a complex circadian response, with exogenous ABA having no effect or increasing the circadian period in plants grown in the presence of Suc (Hanano et al., 2006; Liu et al., 2013). Conversely, ABA shortens the circadian period in the absence of exogenous Suc (Lee et al., 2016). We were able to recapitulate this latter phenotype in wild-type plants under our conditions (grown in the absence of exogenous Suc; Fig. 2H). Similarly, an accelerated FRP was observed in *sal1* seedlings in response to ABA (Fig. 2H), demonstrating that these lines retain a sensitivity to this hormone. Although we cannot completely discount a role for altered ABA signaling in the *sal1* phenotype, we do note that a reduction of PAP accumulation in *sal1* mutants overexpressing *AHL* was sufficient to rescue the *sal1* mutant phenotype (Fig. 4, B–D). Therefore, we propose that the perturbations in plant hormone accumulation and sensitivity in *sal1* alleles are part of the global developmental consequences of increased PAP accumulation, rather than altered ABA sensitivity inducing the extended circadian FRP observed.

Regulation of the Circadian System by SAL1 Does Not Arise as a Consequence of Sulfate Limitation in *sal1*

Sulfate assimilation occurs via a branching pathway, part of which culminates in the production of PAPS that acts as a donor of activated sulfate for many sulfation reactions (Fig. 6A; Takahashi et al., 2011). *sal1* mutants also accumulate desulfo-glucosinolates, presumably because of a homeostatic disruption within this branch

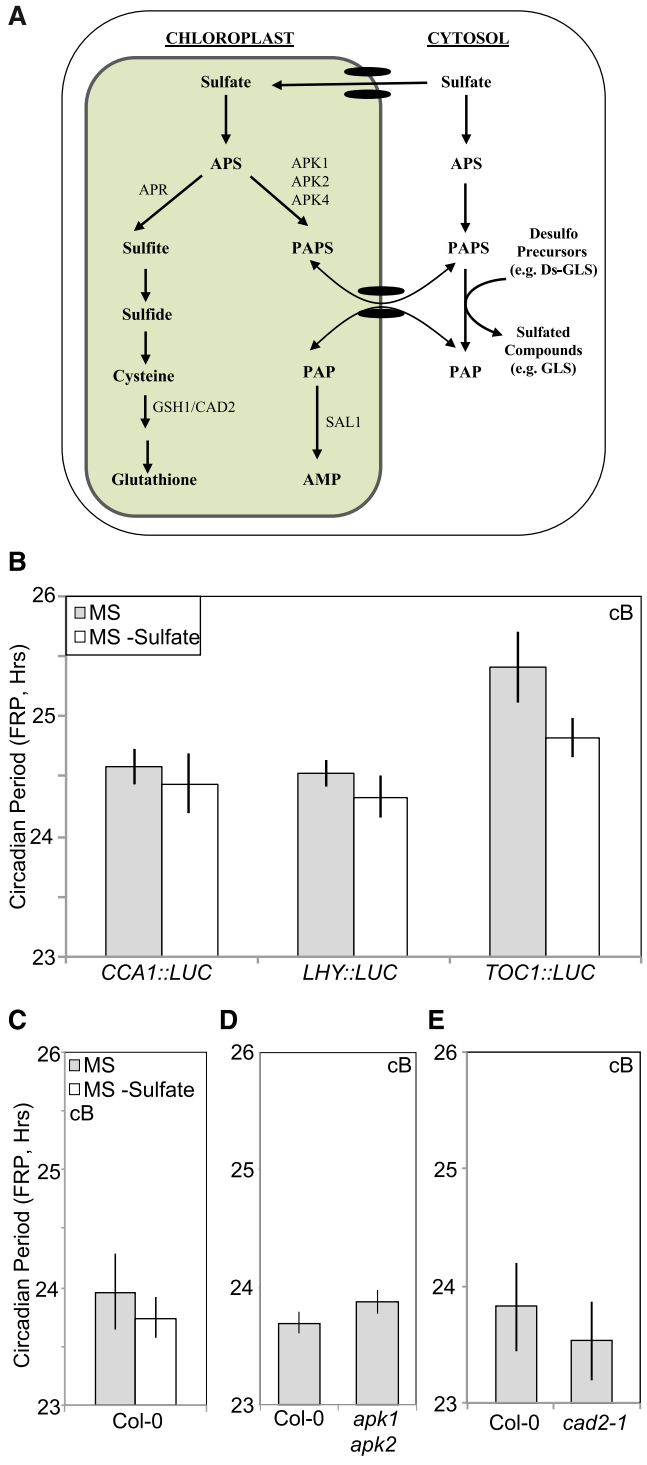

Figure 6. Sulfate deprivation does not extend circadian period. A, Schematic of sulfate metabolism in Arabidopsis, adapted from Bohrer et al. (2015). APS, adenosine-5′-phosphosulfate; GLS, glucosinolate; APK, APS KINASE; APR, APS REDUCTASE; GSH1, GLU-CYS LIGASE. B, Circadian period estimates of luciferase activity in the presence or absence of sulfate salts. Col-0 seedlings carrying either the *CCA1*, *LHY*, or *TOC1* promoters fused to a *LUCIFERASE* reporter were assessed. Plants were entrained for 12 d before transfer to cB light (20 μmol m^{-2} s^{-1}) for imaging. SE is shown, $n = 10$. Data from one of three independent experiments are shown. C, Circadian rhythms of F_q'/F_m' in plants grown on agar lacking sulfate salts. Plants were grown as described in B. Data represent mean values of multiple seedlings ($n = 8$) and are representative of at least three independent experiments. D and E, Circadian period estimates of F_q'/F_m' in *apk1 apk2* (D) and *cad2-1* (E) plants. Data are representative of at least two independent experiments. SE is shown, $n = 8$.

of the sulfate assimilation pathway as a consequence of the accumulation of PAPS and PAP (Lee et al., 2012). Consequently, *sal1* lines also accumulate jasmonic acid (Rodríguez et al., 2010). Previous work has demonstrated that jasmonic acid production is regulated by the circadian system (Goodspeed et al., 2012), and jasmonate signaling is gated by the clock, leading to improved resistance against herbivory and infection (Covington et al., 2008; Goodspeed et al., 2012; Shin et al., 2012; Ingle et al., 2015).

A recent study demonstrated that perturbed glucosinolate accumulation shortens FRP under cR+B light (Kerwin et al., 2011). In order to test the consequences of perturbed sulfate metabolism upon FRP under our experimental conditions, we examined plants grown on sulfate-deficient media (Fig. 6, B and C) and mutants with perturbed sulfate metabolism (*apk1 apk2* and *cad2-1*; Fig. 6, D and E). In agreement with Kerwin et al., we did not observe a significant extension of FRP in sulfate-deprived conditions (Fig. 6, B and C). Instead, we observed a modest shortening of FRP in one of our luciferase lines (*TOC1::LUC*; Fig. 6B). Our data subsequently suggest that sulfate limitation does not induce a long FRP and is not the mechanism by which PAP regulates circadian rhythm.

Loss of XRN Activity Replicates the Circadian Phenotypes of *sal1* Mutants

The importance of posttranscriptional regulation of circadian gene expression is increasingly being recognized, particularly in response to environmental changes (Garbarino-Pico and Green, 2007; Kojima et al., 2011; Sanchez et al., 2011b). Misregulation of RNA processing frequently leads to an altered circadian FRP (Jones et al., 2012; Wang et al., 2012; MacGregor et al., 2013; Perez-Santángelo et al., 2014) and alternate splicing contributes to modifications to the circadian system in response to temperature and drought (James et al., 2012; Filichkin et al., 2015). Similarly, circadian regulation of exosome activity has previously been implicated in the circadian system of the bread mold *Neurospora crassa* (Guo et al., 2009; Zhang et al., 2015).

Inactivation of SAL1 by oxidative stress induces the intracellular accumulation of PAP that inhibits the activity of XRN exoribonucleases (Dichtl et al., 1997; Mechold et al., 2006; Estavillo et al., 2011). Redundancy between *XRN* family members has previously been reported and the accumulated PAP in mutant alleles of *SAL1* have been suggested to simultaneously inhibit all

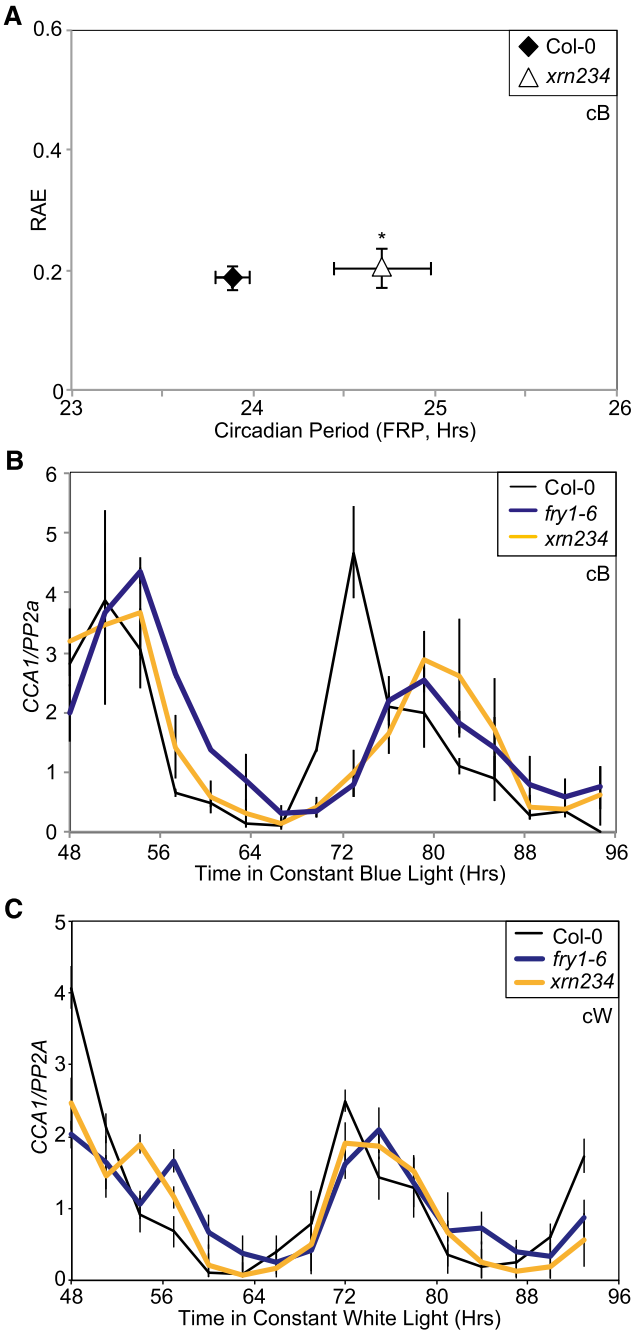

Figure 7. Circadian phenotypes of *xrn* mutants. A, Rhythms of PSII operating efficiency (F_q'/F_m') were measured over circadian time in Col-0 and *xrn2-1 xrn3-3 xrn4-6* (*xrn234*) mutant seedlings. Period estimates are plotted against RAE. Plants were grown for 12 d under 12/12-h L/D cycles before being transferred to cB light (20 μmol m^{-2} s^{-1}). Data represent mean values of multiple seedlings ($n = 7$) and are representative of three independent experiments. Error bars indicate SE, and asterisks indicate a significant difference compared with Col-0 plants ($P < 0.05$, Student's *t* test). B, Assessment of *CCA1* transcript accumulation under cB light in Col-0, *fry1-6*, and *xrn234* seedlings using RT-qPCR. Plants were entrained in 12/12-h L/D cycles before being moved to constant conditions with 20 μmol m^{-2} s^{-1} blue light. Data for each gene were normalized with an internal control (*PP2a*) and are the mean of three biological replicates. C, *CCA1* transcript accumulation under cW light in *fry1-6* and *xrn234* seedlings. Transcript accumulation in Col-0, *fry1-6*, and *xrn234* seedlings was compared using RT-qPCR. Plants were entrained as in B before being moved to constant conditions with 60 μmol m^{-2} s^{-1} white light. Data for each gene were normalized with an internal control (*PP2a*) and are the mean of three biological replicates. Error bars indicate SE.

three XRNs (Gy et al., 2007; Nagarajan et al., 2013). In addition, a role for cytoplasmic XRN activity within the circadian system of the green algae *Chlamydomonas reinhardtii* has been observed (Matsuo et al., 2008). In this case, loss of XRN activity led to a lengthened FRP, similar to that observed in *sal1* and *xrn234* plants (Figs. 2 and 7). Therefore, it is possible that the loss of XRN activity induces global changes in circadian transcript abundance and/or stability that likely account for the delayed FRP of the circadian system.

Osmotic Stress Delays the Circadian System

Many stress responses are typically associated with different times of day, leading to speculation that such responses are modulated by the circadian system (Walley et al., 2007; Mizuno and Yamashino, 2008; Sanchez et al., 2011a; Grundy et al., 2015). While the role of the circadian system in modulating plants' tolerance of water-deprived conditions is beginning to be elucidated (Fukushima et al., 2009; Legnaioli et al., 2009; Wilkins et al., 2010; Nakamichi et al., 2016), comparatively little is understood regarding how osmotic stress influences the circadian system (Grundy et al., 2015). Multiple clock transcripts accumulate to a greater extent in response to osmotic stress in barley (*Hordeum vulgare*), although a consistent change in the phase of gene expression was not observed under diel conditions in this previous work (Habte et al., 2014). One of the consequences of drought and osmotic stress is the increased generation of reactive oxygen species during photosynthesis, leading to changes in the redox state of the chloroplast (Apel and Hirt, 2004; Chan et al., 2016b). Recent work has revealed that the redox status of peroxiredoxins within the chloroplast varies with a circadian rhythm (Edgar et al., 2012), while a similar circadian pattern of H_2O_2 accumulation and catalase activity is also apparent (Lai et al., 2012).

Our work demonstrated that osmotic stress is sufficient to extend circadian period in Arabidopsis under either cR+B, cR, or cB light, although a much more pronounced effect was observed under monochromatic blue light conditions (Figs. 1A and 8, C and D; Supplemental Fig. S7). In addition, the extension of the circadian period was correlated with the accumulation of PAP in wild-type plants (Figs. 1 and 8). While we do not consider plants' perception and response to osmotic stress to occur solely via the regulation of SAL1 activity, it was noteworthy that a significant response to osmotic stress was not observed in *sal1* lines transferred to

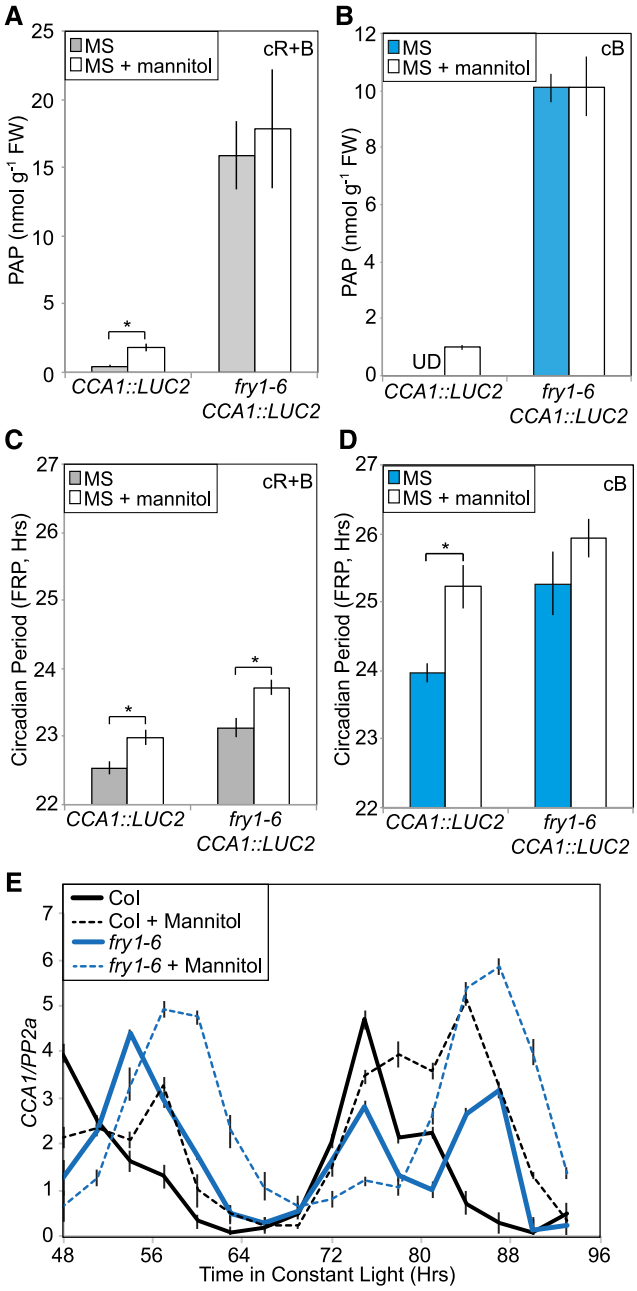

Figure 8. PAP levels correlate with a lengthened circadian period under osmotic stress and broad-spectrum blue light. A and B, Accumulation of PAP in Col-0 and *fry1-6* seedlings in the presence of 200 mM mannitol. Plants were grown for 11 d under 12/12-h L/D cycles before being transferred to plates containing 200 mM mannitol 24 h before transfer to constant light. Plates were subsequently transferred to either constant red and blue light (30 μmol m^{-2} s^{-1} constant red light supplemented with 20 μmol m^{-2} s^{-1} blue light [cR+B]; A) or to 20 μmol m^{-2} s^{-1} cB (B) at dawn of day 12. Seedlings were harvested at ZT96. UD, PAP levels were below the detection threshold. Data are the mean of three biological replicates and are representative of two independent experiments. SD is shown. Asterisks indicate a significant difference compared to a mock-treated control ($P < 0.025$, Bonferroni adjusted Student's *t* test). C and D, Circadian period estimates of luciferase activity in Col-0 and *fry1-6* plants carrying a *CCA1::LUC2* reporter construct in the presence of 200 mM mannitol. Plants were entrained and transferred to growth substrate containing 200 mM mannitol as in A. Seedlings were transferred to either cR+B (C) or cB (D) for imaging. Data are representative of three independent experiments. Error bars express SE, $n = 10$. Asterisks indicate a significant difference compared with a mock-treated control ($P < 0.025$, Bonferroni adjusted Student's *t* test). E, Accumulation of *CCA1* transcript following transfer to 200 mM mannitol. Plants were entrained to 12/12-h L/D cycles for 11 d on MS medium before being transferred to either 200 mM mannitol or a mock treatment at dawn. Seedlings were moved to constant conditions with 20 μmol m^{-2} s^{-1} blue light at dawn of day 12. Data were normalized with an internal control (*PP2a*) and are the mean of at least two biological replicates. Error bars indicate SE.

cB light (Fig. 8D); such data are consistent with the pronounced circadian phenotype of *sal1* alleles, specifically under these conditions (Figs. 2 and 3) and reveal an additional contribution of SAL1 to plants' responses to osmotic stress.

Recently, it has been suggested that a delay of the circadian system acts to slow metabolism, consequently improving survival during suboptimal conditions (Syed et al., 2015). Such data are consistent with our observations that increased levels of PAP (due to the mutation of SAL1 or the application of osmotic stress) lengthens FRP and delays flowering (Figs. 1, 3, 4, and 8; Wilson et al., 2009). Therefore, we propose that the accumulation of PAP in response to environmental stress leads to the inhibition of XRN exoribonucleases, leading to enhanced stability of specific transcripts and a consequent delay in circadian timing. This mechanism enables environmental signals to be integrated with the circadian clock to adjust plants' response to stressful conditions.

MATERIALS AND METHODS

Plant Materials and Growth Conditions

Mutant alleles of *SAL1* have been reported previously (Rossel et al., 2006; Gy et al., 2007; Rodríguez et al., 2010). *alx8-1* and *fry1-6* alleles of *SAL1* were reisolated from seed provided by the Nottingham Arabidopsis Stock Centre (Scholl et al., 2000). The *xrn2-1 xrn3-3 xrn4-6* triple mutant has previously been reported (Hirsch et al., 2011). *apk1 apk2* lines were a kind gift from the Farmer lab (University of Lausanne, Switzerland; Rodríguez et al., 2010). *cad2-1* seeds (Cobbett et al., 1998) were provided by Prof. Phil Mullineaux (University of Essex, UK). *fry1-6 CCA1::LUC2* lines were generated by crossing *fry1-6* to a previously reported Columbia *CCA1::LUC2* line (Jones et al., 2015). Transgenic plants were generated as follows. The *SAL1* coding sequence and a 900-bp region upstream of the transcriptional start site were transferred into pCR8/GW/TOPO (Invitrogen) via the TOPO cloning method using oligonucleotides described in Supplemental Table S1. A binary vector containing this *SAL1* genomic fragment was created by LR recombination with pGWB4 (Nakagawa et al., 2007) to generate pGWB4 SAL1. The *AHL* coding sequence was similarly transferred into pCR8/GW/TOPO using oligonucleotides described in Supplemental Table S1. A binary vector containing the *AHL* cDNA fragment was created by LR recombination with pGWB41 (Nakagawa et al., 2007) to generate pGWB41 AHL. Plasmids were moved into *Agrobacterium tumefaciens* strain GV3101 and transformed into *alx8-1* plants using standard protocols (Narusaka et al., 2010). Transformants were selected on MS media supplemented with 50 μg/mL hygromycin (Fisher Scientific).

All wild-type and transgenic lines were in the Arabidopsis (*Arabidopsis thaliana*) ecotype Columbia-0 (Col-0) background. Seeds were surface sterilized

and sown on soil or 0.8% agar plates containing half-strength MS medium (Sigma-Aldrich M5524). For sulfate deficiency experiments, sulfate salts in MS medium M5524 (http://www.sigmaaldrich.com/technical-documents/protocols/biology/murashige-skoog.html) were replaced with chloride salts as follows: 10.31 mM NH_4NO_3, 0.05 mM H_3BO_3, 1.50 mM $CaCl_2$, 0.05 ρM $CoCl_2$, 0.05 ρM $CuCl_2$, 0.05 mM EDTA, 0.05 mM $FeCl_3$, 0.75 mM $MgCl_2$, 0.05 mM $MnCl_2$, 0.52 ρM Na_2MoO_4, 2.50 ρM KI, 9.40 mM KNO_3, 0.63 mM KH_2PO_4, 15 ρM $ZnCl_2$, and 0.8% agar, pH 5.7. Plants were entrained under 12-h-white-light/12-h-dark cycles.

Application of Osmotic Stress

In order to apply osmotic stress (−0.5 MPa), 5-d-old seedlings were transferred from MS plates to those containing either osmotica 24 h before transfer to constant light for imaging. Treatment plates contained either 200 mM mannitol or were infused with PEG 8000 as described by Verslues et al. (2006). In brief, 1.5% agar plates containing half-strength MS medium and 6 mM MES buffer were solidified and then overlaid with a solution of 250 g/L PEG 8000. The solution was allowed to sit for 24 h, producing an osmotic potential of −0.5 MPa, before the excess solution was removed from the plates prior to transplant.

Luciferase Imaging

To complete luciferase imaging, individual seedlings were entrained for 6 d in 12-h/12-h light/dark cycles under white light on half-strength MS media without supplemental Suc (unless transferred to constant darkness, in which case 3% [w/v] Suc was added to the media). Plants were sprayed with 3 mM D-luciferin in 0.01% Triton X-100 before being transferred to free-running conditions under the indicated fluence rate as previously described (Litthauer et al., 2015). Data were processed using ImageJ software (Schneider et al., 2012). Patterns of bioluminescence were fitted to cosine waves using Fourier fast transform-nonlinear least squares (FFT-NLLS; Plautz et al., 1997) to estimate the length of the circadian period. Relative amplitude error (RAE) is a measure of rhythmic robustness, with a value of 0 indicating an exact fit to a cosine wave (Plautz et al., 1997). Sample size was chosen to achieve a power of 0.8 in a two-sample t test at $\alpha = 0.05$. Previously collected data were used to estimate $\sigma = 0.6$.

Abscisic Acid Treatment

Six-day-old seedlings were entrained for luciferase imaging (as described above) before being transplanted to half-strength MS media plates containing either 10 μM abscisic acid (Acros Organics 133485000) or a mock treatment (0.1% DMSO) at dawn (Zeitgeber [ZT] 0). Plants were sprayed with 3 mM D-luciferin in 0.01% Triton X-100 before being transferred to free-running conditions under a combination of 30 μmol m^{-2} s^{-1} red light and 20 μmol m^{-2} s^{-1} blue light for circadian imaging.

Methyl Viologen Treatment

Six-day-old seedlings were entrained for luciferase imaging (as described above) before being sprayed with 50 μM methyl viologen (Sigma-Aldrich) and 3 mM D-luciferin in 0.01% Triton X-100 at dawn (ZT0). Plants were transferred to free-running conditions under a combination of 30 μmol m^{-2} s^{-1} red light and 20 μmol m^{-2} s^{-1} blue light for circadian imaging.

Application of PAP to Seedlings

Twelve-day-old seedlings were prepared for luciferase imaging (as described above) and transferred into constant blue light (20 μmol m^{-2} s^{-1}). PAP (1 mM) was applied to seedlings in 0.01% Triton X-100 at ZT29. Luciferase imaging and circadian analysis was completed as described above.

Chlorophyll Fluorescence Imaging

Chlorophyll fluorescence parameters were recorded with a Fluorimager imaging system (Technologica) as previously described (Litthauer et al., 2015). Patterns of F_q'/F_m' were fitted to cosine waves using FFT-NLLS (Plautz et al., 1997) to estimate circadian period length and additional circadian parameters. Sample size was chosen to achieve a power of 0.8 in a two-sample t test at $\alpha = 0.05$. Previously collected data were used to estimate $\sigma = 0.6$.

RT-qPCR

Following entrainment, plants were transferred to constant light at the indicated fluence rate and quality. Tissue was harvested at the indicated time directly onto liquid nitrogen before RNA was isolated from 10 to 15 seedlings for each data point using Tri Reagent according to the manufacturer's protocol (Sigma-Aldrich). Reverse transcription was performed using RevertAid reverse transcriptase following DNase treatment (Fisher Scientific). RT-qPCR was performed using a Bio-Rad CFX96 Real-Time system following MIQE guidelines (Bustin et al., 2009). PCR was completed for 40 cycles using the following protocol: 95°C for 15 s, 55°C for 15 s, and 72°C for 30 s. Each biological sample was run in triplicate, with starting quantity estimated from critical thresholds using the standard curve of amplification using Bio-Rad CFX Manager 5.1. Calibration curves were run as an internal control within each RT-qPCR run, with data only accepted if experimental samples fell within the linear range of amplification, and if quality criteria were met ($r^2 > 0.97$, PCR efficiency ± 15%, as determined from the calibration curve). Data for each sample were normalized to *PP2A* as an internal control. Primer sets used are described in Supplemental Table S1.

Protein Extraction and Immunoblot Analysis

Twelve-day-old seedlings were frozen in liquid nitrogen, ground into powder, and extracted in homogenization buffer (25 mM MOPS, 0.25 M Suc, 0.1 mM $MgCl_2$, and 8 mM L-Cys, pH 7.8). After quantifying the total protein concentrations with Bradford Reagent (Sigma-Aldrich), equal amounts of proteins were separated on 12.5% SDS-PAGE gels and then semidry transferred onto a 0.45 μM nitrocellulose membrane (Amersham). SAL1-GFP and actin were immunodetected by anti-GFP (Ab290, 1:10,000 dilution; Abcam) and antiactin (mAB1501, 1:2,000; Sigma-Aldrich) antibodies, respectively. IgG (H+L) HRP conjugates (Promega) were used to detect the primary antibodies. Immunoreactive bands were quantified by scanning the membrane with a Fusion FX imaging system (Vilber Lourmat).

Extraction and HPLC Analysis of PAP

PAP was extracted from whole seedlings as previously described (Bürstenbinder et al., 2007; Estavillo et al., 2011). Metabolites were extracted from 150 to 300 mg ground tissue using 1 mL 0.1 M HCl with incubation on ice for 15 min and centrifuged twice at 16,000*g* at 4°C for 5 min. The supernatant (150 μL) was added to 770 μL CP buffer (620 mM citric acid and 760 mM Na_2HPO_4, pH 4) and derivatized using 80 μL 50% (w/v) chloroacetaldehyde solution with incubation at 80°C for 10 min, and centrifuged for 45 min at 16,000*g* at 4°C. Analysis of PAP was performed as previously described (Bürstenbinder et al., 2007; Estavillo et al., 2011). Twenty microliters of the supernatant was injected into an Agilent 1100 HPLC system connected to a FLD G1321A (Agilent) fluorescent detector. PAP was analyzed by reverse-phase HPLC using a Luna 5 μm C18(2) 100 Å column (Phenomenex). The column was equilibrated for 0.2 min with 95% (v/v) of buffer A (5.7mM $[CH_3(CH_2)_3]_4NHSO_4$ and 30.5 mM KH_2PO_4, pH 5.8) and 5% (v/v) buffer B (67% [v/v] acetonitrile and 33% [v/v] buffer A), followed by a linear gradient for 53 min up to 50% (v/v) of buffer B. The column was reequilibrated for 7 min with 5% (v/v) buffer B. PAP concentration was calculated relative to a commercially available standard (Santa Cruz Biotechnology; sc-210760).

Accession Numbers

Genes examined in this article can be found in the Arabidopsis Genome Initiative database under the following accession numbers: *APK1*, At2g14750; *APK2*, At4g39940; *AHL*, At5g54390; *CAD2/GSH1*, At4g23100; *CCA1*, At2g46830; *CRY1*, At4g08920; *CRY2*, At1g04400; *ELF4*, At2g40080; *GIGANTEA*, At1g22770; *LHY*, At1g01060; *PRR5*, At5g24470; *SAL1*, At5g63980; *TOC1*, At5g61380; XRN2, At5g42540; *XRN3*, At1g75660; *XRN4*, At1g54490; and *ZTL*, At5g57360.

Supplemental Data

The following supplemental materials are available.

Supplemental Figure S1. *sal1* alleles have an extended circadian period.

Supplemental Figure S2. Abundance of clock transcripts in *sal1* seedlings.

Supplemental Figure S3. Abundance of blue photoreceptors in *sal1* seedlings.

Supplemental Figure S4. PAP accumulation under constant red light.

Supplemental Figure S5. Transcript accumulation of *SAL1* and *XRN* ribonucleases in entraining and constantly lit conditions.

Supplemental Figure S6. Sulfate deprivation induces the accumulation of genes associated with sulfur anabolism.

Supplemental Figure S7. Circadian rhythms in response to osmotic stress under constant red light.

Supplemental Figure S8. Abundance of clock transcripts in response to osmotic stress.

Supplemental Table S1. Oligos used in this study.

ACKNOWLEDGMENTS

We thank Prof. Barry Pogson (ANU, Australia) and Dr. Markus Wirtz (Universitat Heidelberg), as well as Drs. Uli Bechold and Stuart Fisk (University of Essex) for useful discussions. We thank Prof. Edward Farmer (University of Lausanne, Switzerland), Drs. Pascal Genschik and Thomas Potuschak (CNRS, France), Prof. Antony Hall (Earlham Institute, UK), Prof. Phil Mullineaux (University of Essex, UK), Prof. Albrecht von Arnim (University of Tennessee), and Prof. Alex Webb (University of Cambridge, UK) for providing seeds.

Received November 8, 2017; accepted February 19, 2018; published February 27, 2018.

LITERATURE CITED

Adams S, Manfield I, Stockley P, Carré IA (2015) Revised morning loops of the Arabidopsis circadian clock based on analyses of direct regulatory interactions. PLoS One **10:** e0143943

Alabadí D, Oyama T, Yanovsky MJ, Harmon FG, Más P, Kay SA (2001) Reciprocal regulation between TOC1 and LHY/CCA1 within the Arabidopsis circadian clock. Science **293:** 880–883

Apel K, Hirt H (2004) Reactive oxygen species: metabolism, oxidative stress, and signal transduction. Annu Rev Plant Biol **55:** 373–399

Bohrer A-S, Kopriva S, Takahashi H (2015) Plastid-cytosol partitioning and integration of metabolic pathways for APS/PAPS biosynthesis in *Arabidopsis thaliana*. Front Plant Sci **5:** 751

Bustin SA, Benes V, Garson JA, Hellemans J, Huggett J, Kubista M, Mueller R, Nolan T, Pfaffl MW, Shipley GL, Vandesompele J, Wittwer CT (2009) The MIQE guidelines: minimum information for publication of quantitative real-time PCR experiments. Clin Chem **55:** 611–622

Bürstenbinder K, Rzewuski G, Wirtz M, Hell R, Sauter M (2007) The role of methionine recycling for ethylene synthesis in Arabidopsis. Plant J **49:** 238–249

Chan KX, Mabbitt PD, Phua SY, Mueller JW, Nisar N, Gigolashvili T, Stroeher E, Grassl J, Arlt W, Estavillo GM, Jackson CJ, Pogson BJ (2016a) Sensing and signaling of oxidative stress in chloroplasts by inactivation of the SAL1 phosphoadenosine phosphatase. Proc Natl Acad Sci USA **113:** E4567–E4576

Chan KX, Phua SY, Crisp P, McQuinn R, Pogson BJ (2016b) Learning the languages of the chloroplast: retrograde signaling and beyond. Annu Rev Plant Biol **67:** 25–53

Chen H, Xiong L (2010) The bifunctional abiotic stress signalling regulator and endogenous RNA silencing suppressor FIERY1 is required for lateral root formation. Plant Cell Environ **33:** 2180–2190

Chen H, Zhang B, Hicks LM, Xiong L (2011) A nucleotide metabolite controls stress-responsive gene expression and plant development. PLoS One **6:** e26661

Chen Y-Y, Wang Y, Shin L-J, Wu J-F, Shanmugam V, Tsednee M, Lo J-C, Chen C-C, Wu S-H, Yeh K-C (2013) Iron is involved in the maintenance of circadian period length in Arabidopsis. Plant Physiol **161:** 1409–1420

Chow BY, Helfer A, Nusinow DA, Kay SA (2012) ELF3 recruitment to the PRR9 promoter requires other Evening Complex members in the Arabidopsis circadian clock. Plant Signal Behav **7:** 170–173

Cobbett CS, May MJ, Howden R, Rolls B (1998) The glutathione-deficient, cadmium-sensitive mutant, cad2-1, of *Arabidopsis thaliana* is deficient in gamma-glutamylcysteine synthetase. Plant J **16:** 73–78

Covington MF, Maloof JN, Straume M, Kay SA, Harmer SL (2008) Global transcriptome analysis reveals circadian regulation of key pathways in plant growth and development. Genome Biol **9:** R130

Dichtl B, Stevens A, Tollervey D (1997) Lithium toxicity in yeast is due to the inhibition of RNA processing enzymes. EMBO J **16:** 7184–7195

Dong MA, Farré EM, Thomashow MF (2011) Circadian clock-associated 1 and late elongated hypocotyl regulate expression of the C-repeat binding factor (CBF) pathway in Arabidopsis. Proc Natl Acad Sci USA **108:** 7241–7246

Edgar RS, Green EW, Zhao Y, van Ooijen G, Olmedo M, Qin X, Xu Y, Pan M, Valekunja UK, Feeney KA, Maywood ES, Hastings MH, et al (2012) Peroxiredoxins are conserved markers of circadian rhythms. Nature **485:** 459–464

Eriksson ME, Webb AAR (2011) Plant cell responses to cold are all about timing. Curr Opin Plant Biol **14:** 731–737

Estavillo GM, Crisp PA, Pornsiriwong W, Wirtz M, Collinge D, Carrie C, Giraud E, Whelan J, David P, Javot H, et al (2011) Evidence for a SAL1-PAP chloroplast retrograde pathway that functions in drought and high light signaling in Arabidopsis. Plant Cell **23:** 3992–4012

Fankhauser C, Staiger D (2002) Photoreceptors in *Arabidopsis thaliana*: light perception, signal transduction and entrainment of the endogenous clock. Planta **216:** 1–16

Farré EM, Kay SA (2007) PRR7 protein levels are regulated by light and the circadian clock in Arabidopsis. Plant J **52:** 548–560

Filichkin SA, Cumbie JS, Dharmawardhana P, Jaiswal P, Chang JH, Palusa SG, Reddy ASN, Megraw M, Mockler TC (2015) Environmental stresses modulate abundance and timing of alternatively spliced circadian transcripts in Arabidopsis. Mol Plant **8:** 207–227

Fukushima A, Kusano M, Nakamichi N, Kobayashi M, Hayashi N, Sakakibara H, Mizuno T, Saito K (2009) Impact of clock-associated Arabidopsis pseudo-response regulators in metabolic coordination. Proc Natl Acad Sci USA **106:** 7251–7256

Garbarino-Pico E, Green CB (2007) Posttranscriptional regulation of mammalian circadian clock output. Cold Spring Harb Symp Quant Biol **72:** 145–156

Gendron JM, Pruneda-Paz JL, Doherty CJ, Gross AM, Kang SE, Kay SA (2012) Arabidopsis circadian clock protein, TOC1, is a DNA-binding transcription factor. Proc Natl Acad Sci USA **109:** 3167–3172

Goodspeed D, Chehab EW, Min-Venditti A, Braam J, Covington MF (2012) Arabidopsis synchronizes jasmonate-mediated defense with insect circadian behavior. Proc Natl Acad Sci USA **109:** 4674–4677

Grundy J, Stoker C, Carré IA (2015) Circadian regulation of abiotic stress tolerance in plants. Front Plant Sci **6:** 648

Guo J, Cheng P, Yuan H, Liu Y (2009) The exosome regulates circadian gene expression in a posttranscriptional negative feedback loop. Cell **138:** 1236–1246

Gy I, Gasciolli V, Lauressergues D, Morel J-B, Gombert J, Proux F, Proux C, Vaucheret H, Mallory AC (2007) Arabidopsis FIERY1, XRN2, and XRN3 are endogenous RNA silencing suppressors. Plant Cell **19:** 3451–3461

Habte E, Müller LM, Shtaya M, Davis SJ, von Korff M (2014) Osmotic stress at the barley root affects expression of circadian clock genes in the shoot. Plant Cell Environ **37:** 1321–1327

Hanano S, Domagalska MA, Nagy F, Davis SJ (2006) Multiple phytohormones influence distinct parameters of the plant circadian clock. Genes Cells **11:** 1381–1392

Herrero E, Kolmos E, Bujdoso N, Yuan Y, Wang M, Berns MC, Uhlworm H, Coupland G, Saini R, Jaskolski M, et al (2012) EARLY FLOWERING4 recruitment of EARLY FLOWERING3 in the nucleus sustains the Arabidopsis circadian clock. Plant Cell **24:** 428–443

Hirsch J, Misson J, Crisp PA, David P, Bayle V, Estavillo GM, Javot H, Chiarenza S, Mallory AC, Maizel A, et al (2011) A novel fry1 allele reveals the existence of a mutant phenotype unrelated to 5′->3′ exoribonuclease (XRN) activities in *Arabidopsis thaliana* roots. PLoS One **6:** e16724

Hong S, Kim SA, Guerinot ML, McClung CR (2013) Reciprocal interaction of the circadian clock with the iron homeostasis network in Arabidopsis. Plant Physiol **161:** 893–903

Hsu PY, Harmer SL (2014) Wheels within wheels: the plant circadian system. Trends Plant Sci **19:** 240–249

Huang W, Pérez-García P, Pokhilko A, Millar AJ, Antoshechkin I, Riechmann JL, Mas P (2012) Mapping the core of the Arabidopsis circadian clock defines the network structure of the oscillator. Science **336:** 75–79

Hut RA, Beersma DGM (2011) Evolution of time-keeping mechanisms: early emergence and adaptation to photoperiod. Philos Trans R Soc Lond B Biol Sci **366:** 2141–2154

Ingle RA, Stoker C, Stone W, Adams N, Smith R, Grant M, Carré I, Roden LC, Denby KJ (2015) Jasmonate signalling drives time-of-day differences in susceptibility of Arabidopsis to the fungal pathogen *Botrytis cinerea*. Plant J **84:** 937–948

James AB, Syed NH, Bordage S, Marshall J, Nimmo GA, Jenkins GI, Herzyk P, Brown JWS, Nimmo HG (2012) Alternative splicing mediates responses of the Arabidopsis circadian clock to temperature changes. Plant Cell **24:** 961–981

Jones M (2009) Entrainment of the Arabidopsis circadian clock. J Plant Biol **52:** 202–209

Jones M (2017) Interplay of Circadian Rhythms and Light in the Regulation of Photosynthesis-Derived Metabolism. Progress in Botany **79:** 147–171

Jones MA, Hu W, Litthauer S, Lagarias JC, Harmer SL (2015) A constitutively active allele of phytochrome B maintains circadian robustness in the absence of light. Plant Physiol **169:** 814–825

Jones MA, Williams BA, McNicol J, Simpson CG, Brown JWS, Harmer SL (2012) Mutation of Arabidopsis spliceosomal timekeeper locus1 causes circadian clock defects. Plant Cell **24:** 4066–4082

Kastenmayer JP, Green PJ (2000) Novel features of the XRN-family in Arabidopsis: evidence that AtXRN4, one of several orthologs of nuclear Xrn2p/Rat1p, functions in the cytoplasm. Proc Natl Acad Sci USA **97:** 13985–13990

Kerwin RE, Jiménez-Gómez JM, Fulop D, Harmer SL, Maloof JN, Kliebenstein DJ (2011) Network quantitative trait loci mapping of circadian clock outputs identifies metabolic pathway-to-clock linkages in Arabidopsis. Plant Cell **23:** 471–485

Kim B-H, von Arnim AG (2009) FIERY1 regulates light-mediated repression of cell elongation and flowering time via its 3′(2′),5′-bisphosphate nucleotidase activity. Plant J **58:** 208–219

Kojima S, Shingle DL, Green CB (2011) Post-transcriptional control of circadian rhythms. J Cell Sci **124:** 311–320

Kurihara Y, Schmitz RJ, Nery JR, Schultz MD, Okubo-Kurihara E, Morosawa T, Tanaka M, Toyoda T, Seki M, Ecker JR (2012) Surveillance of 3′ noncoding transcripts requires FIERY1 and XRN3 in Arabidopsis. G3 (Bethesda) **2:** 487–498

Lai AG, Doherty CJ, Mueller-Roeber B, Kay SA, Schippers JHM, Dijkwel PP (2012) CIRCADIAN CLOCK-ASSOCIATED 1 regulates ROS homeostasis and oxidative stress responses. Proc Natl Acad Sci USA **109:** 17129–17134

Lee B-R, Huseby S, Koprivova A, Chételat A, Wirtz M, Mugford ST, Navid E, Brearley C, Saha S, Mithen R, et al (2012) Effects of fou8/fry1 mutation on sulfur metabolism: is decreased internal sulfate the trigger of sulfate starvation response? PLoS One **7:** e39425

Lee HG, Más P, Seo PJ (2016) MYB96 shapes the circadian gating of ABA signaling in Arabidopsis. Sci Rep **6:** 17754

Legnaioli T, Cuevas J, Más P (2009) TOC1 functions as a molecular switch connecting the circadian clock with plant responses to drought. EMBO J **28:** 3745–3757

Litthauer S, Battle MW, Lawson T, Jones MA (2015) Phototropins maintain robust circadian oscillation of PSII operating efficiency under blue light. Plant J **83:** 1034–1045

Liu T, Carlsson J, Takeuchi T, Newton L, Farré EM (2013) Direct regulation of abiotic responses by the Arabidopsis circadian clock component PRR7. Plant J **76:** 101–114

Lu SX, Webb CJ, Knowles SM, Kim SHJ, Wang Z, Tobin EM (2012) CCA1 and ELF3 Interact in the control of hypocotyl length and flowering time in Arabidopsis. Plant Physiol **158:** 1079–1088

MacGregor DR, Gould P, Foreman J, Griffiths J, Bird S, Page R, Stewart K, Steel G, Young J, Paszkiewicz K, et al (2013) HIGH EXPRESSION OF OSMOTICALLY RESPONSIVE GENES1 is required for circadian periodicity through the promotion of nucleo-cytoplasmic mRNA export in Arabidopsis. Plant Cell **25:** 4391–4404

Matsuo T, Okamoto K, Onai K, Niwa Y, Shimogawara K, Ishiura M (2008) A systematic forward genetic analysis identified components of the Chlamydomonas circadian system. Genes Dev **22:** 918–930

McWatters HG, Kolmos E, Hall A, Doyle MR, Amasino RM, Gyula P, Nagy F, Millar AJ, Davis SJ (2007) ELF4 is required for oscillatory properties of the circadian clock. Plant Physiol **144:** 391–401

Mechold U, Ogryzko V, Ngo S, Danchin A (2006) Oligoribonuclease is a common downstream target of lithium-induced pAp accumulation in *Escherichia coli* and human cells. Nucleic Acids Res **34:** 2364–2373

Millar AJ (2016) The intracellular dynamics of circadian clocks reach for the light of ecology and evolution. Annu Rev Plant Biol **67:** 595–618

Mittler R, Vanderauwera S, Suzuki N, Miller G, Tognetti VB, Vandepoele K, Gollery M, Shulaev V, Van Breusegem F (2011) ROS signaling: the new wave? Trends Plant Sci **16:** 300–309

Mizuno T, Yamashino T (2008) Comparative transcriptome of diurnally oscillating genes and hormone-responsive genes in *Arabidopsis thaliana*: insight into circadian clock-controlled daily responses to common ambient stresses in plants. Plant Cell Physiol **49:** 481–487

Mockler TC, Michael TP, Priest HD, Shen R, Sullivan CM, Givan SA, McEntee C, Kay SA, Chory J (2007) The DIURNAL project: DIURNAL and circadian expression profiling, model-based pattern matching, and promoter analysis. Cold Spring Harb Symp Quant Biol **72:** 353–363

Mugford SG, Yoshimoto N, Reichelt M, Wirtz M, Hill L, Mugford ST, Nakazato Y, Noji M, Takahashi H, Kramell R, et al (2009) Disruption of adenosine-5′-phosphosulfate kinase in Arabidopsis reduces levels of sulfated secondary metabolites. Plant Cell **21:** 910–927

Nagarajan VK, Jones CI, Newbury SF, Green PJ (2013) XRN 5′→3′ exoribonucleases: structure, mechanisms and functions. Biochim Biophys Acta **1829:** 590–603

Nakagawa T, Kurose T, Hino T, Tanaka K, Kawamukai M, Niwa Y, Toyooka K, Matsuoka K, Jinbo T, Kimura T (2007) Development of series of gateway binary vectors, pGWBs, for realizing efficient construction of fusion genes for plant transformation. J Biosci Bioeng **104:** 34–41

Nakamichi N, Kiba T, Henriques R, Mizuno T, Chua N-H, Sakakibara H (2010) PSEUDO-RESPONSE REGULATORS 9, 7, and 5 are transcriptional repressors in the Arabidopsis circadian clock. Plant Cell **22:** 594–605

Nakamichi N, Takao S, Kudo T, Kiba T, Wang Y, Kinoshita T, Sakakibara H (2016) Improvement of Arabidopsis biomass and cold-, drought-, and salinity-stress tolerance by modified circadian clock-associated PSEUDO-RESPONSE REGULATORs. Plant Cell Physiol **57:** 1085–1097

Narusaka M, Shiraishi T, Iwabuchi M, Narusaka Y (2010) The floral inoculating protocol: a simplified Arabidopsis thaliana transformation method modified from floral dipping. Plant Biotechnol **27:** 349–351

Norén L, Kindgren P, Stachula P, Rühl M, Eriksson ME, Hurry V, Strand Å (2016) Circadian and plastid signaling pathways are integrated to ensure correct expression of the CBF and COR genes during photoperiodic growth. Plant Physiol **171:** 1392–1406

Nusinow DA, Helfer A, Hamilton EE, King JJ, Imaizumi T, Schultz TF, Farré EM, Kay SA (2011) The ELF4-ELF3-LUX complex links the circadian clock to diurnal control of hypocotyl growth. Nature **475:** 398–402

Perez-Santángelo S, Mancini E, Francey LJ, Schlaen RG, Chernomoretz A, Hogenesch JB, Yanovsky MJ (2014) Role for LSM genes in the regulation of circadian rhythms. Proc Natl Acad Sci USA **111:** 15166–15171

Plautz JD, Straume M, Stanewsky R, Jamison CF, Brandes C, Dowse HB, Hall JC, Kay SA (1997) Quantitative analysis of Drosophila period gene transcription in living animals. J Biol Rhythms **12:** 204–217

Pornsiriwong W, Estavillo GM, Chan KX, Tee EE, Ganguly D, Crisp PA, Phua SY, Zhao C, Qiu J, Park J, et al (2017) A chloroplast retrograde signal, 3′-phosphoadenosine 5′-phosphate, acts as a secondary messenger in abscisic acid signaling in stomatal closure and germination. eLife **6:** e23361

Quintero FJ, Garciadeblás B, Rodríguez-Navarro A (1996) The SAL1 gene of Arabidopsis, encoding an enzyme with 3′(2′),5′-bisphosphate nucleotidase and inositol polyphosphate 1-phosphatase activities, increases salt tolerance in yeast. Plant Cell **8:** 529–537

Rodríguez VM, Chételat A, Majcherczyk P, Farmer EE (2010) Chloroplastic phosphoadenosine phosphosulfate metabolism regulates basal levels of the prohormone jasmonic acid in Arabidopsis leaves. Plant Physiol **152:** 1335–1345

Rossel JB, Walter PB, Hendrickson L, Chow WS, Poole A, Mullineaux PM, Pogson BJ (2006) A mutation affecting ASCORBATE PEROXIDASE 2 gene expression reveals a link between responses to high light and drought tolerance. Plant Cell Environ **29:** 269–281

Salomé PA, Oliva M, Weigel D, Krämer U (2013) Circadian clock adjustment to plant iron status depends on chloroplast and phytochrome function. EMBO J **32:** 511–523

Sanchez A, Shin J, Davis SJ (2011a) Abiotic stress and the plant circadian clock. Plant Signal Behav **6:** 223–231

Sanchez SE, Petrillo E, Kornblihtt AR, Yanovsky MJ (2011b) Alternative splicing at the right time. RNA Biol **8:** 954–959

Schneider CA, Rasband WS, Eliceiri KW (2012) NIH Image to ImageJ: 25 years of image analysis. Nat Methods **9:** 671–675

Scholl RL, May ST, Ware DH (2000) Seed and molecular resources for Arabidopsis. Plant Physiol **124:** 1477–1480

Shin J, Heidrich K, Sanchez-Villarreal A, Parker JE, Davis SJ (2012) TIME FOR COFFEE represses accumulation of the MYC2 transcription factor to provide time-of-day regulation of jasmonate signaling in Arabidopsis. Plant Cell **24:** 2470–2482

Song YH, Shim JS, Kinmonth-Schultz HA, Imaizumi T (2015) Photoperiodic flowering: time measurement mechanisms in leaves. Annu Rev Plant Biol **66:** 441–464

Steduto P, Faurès JM, Hoogeveen J (2012) Coping with Water Scarcity: An Action Framework for Agriculture and Food Security. FAO Water Reports **16**: 78

Syed NH, Prince SJ, Mutava RN, Patil G, Li S, Chen W, Babu V, Joshi T, Khan S, Nguyen HT (2015) Core clock, SUB1, and ABAR genes mediate flooding and drought responses via alternative splicing in soybean. J Exp Bot **66:** 7129–7149

Takahashi H, Kopriva S, Giordano M, Saito K, Hell R (2011) Sulfur assimilation in photosynthetic organisms: molecular functions and regulations of transporters and assimilatory enzymes. Annu Rev Plant Biol **62:** 157–184

Terry N (1976) Effects of sulfur on the photosynthesis of intact leaves and isolated chloroplasts of sugar beets. Plant Physiol **57:** 477–479

Verslues PE, Agarwal M, Katiyar-Agarwal S, Zhu J, Zhu J-K (2006) Methods and concepts in quantifying resistance to drought, salt and freezing, abiotic stresses that affect plant water status. Plant J **45:** 523–539

Walley JW, Coughlan S, Hudson ME, Covington MF, Kaspi R, Banu G, Harmer SL, Dehesh K (2007) Mechanical stress induces biotic and abiotic stress responses via a novel cis-element. PLoS Genet **3:** 1800–1812

Wang X, Wu F, Xie Q, Wang H, Wang Y, Yue Y, Gahura O, Ma S, Liu L, Cao Y, et al (2012) SKIP is a component of the spliceosome linking alternative splicing and the circadian clock in Arabidopsis. Plant Cell **24:** 3278–3295

Wilkins O, Bräutigam K, Campbell MM (2010) Time of day shapes Arabidopsis drought transcriptomes. Plant J **63:** 715–727

Wilson PB, Estavillo GM, Field KJ, Pornsiriwong W, Carroll AJ, Howell KA, Woo NS, Lake JA, Smith SM, Harvey Millar A, von Caemmerer S, Pogson BJ (2009) The nucleotidase/phosphatase SAL1 is a negative regulator of drought tolerance in Arabidopsis. Plant J **58:** 299–317

Xiong L, Lee Bh, Ishitani M, Lee H, Zhang C, Zhu J-K (2001) FIERY1 encoding an inositol polyphosphate 1-phosphatase is a negative regulator of abscisic acid and stress signaling in Arabidopsis. Genes Dev **15:** 1971–1984

Zhang L, Wan Y, Huang G, Wang D, Yu X, Huang G, Guo J (2015) The exosome controls alternative splicing by mediating the gene expression and assembly of the spliceosome complex. Sci Rep **5:** 13403